The results of 2005 beam development run.

Maxim A. Bychkov

January 30, 2006

Version 2.0

1 Introduction

October 2005 beam development run is a part of the precise $\pi^+ \to e^+\nu$ branching ratio measurement conducted by the PEN collaboration. The main objectives of this run were:

- Find the optimal momentum of the beam which satisfies the following conditions:
  - Significant TOF separation between the constituents of the beam (positrons, muons and pions).
  - Energy deposited by pions in the target is comparable with the energy deposited by the decay positrons and muons.
  - The intensity of the beam is of the order of 20 KHz with well collimated beam.
- Understand the ADC spectra of the pions, positrons and muons in the target and NaI calorimeter.
- Implement a simple digitizer system and reconstruct $\pi^+ \to e^+\nu$ events from the digitizer waveform information.

For the first part of the 2005 run we have used a simple setup. It consisted of 3 active beam detectors and a set of three quadrupole magnets. Active beam detectors are B0 counter, degrader and target. All three are plastic

scintillators of 2 mm, 5 mm and 15 mm thickness respectively. The separation between the back face of the B0 and the front face of the degrader was 3515 mm and the quadrupole triplet was placed between the B0 and the degrader. The target was 10 mm behind the degrader. A single crystal NaI calorimeter was placed behind the target at the distance of 510 mm and at the angle of 40° with the beam axis. The acceptance defining 10 mm thick plastic, called counter6, is placed at the front face of the NaI calorimeter. Readers referred to pages 99 and 105 of the experiment logbook for the detailed information about the detectors separation and ADC/TDC channel assignment.

2 Method and Results

The first task was to measure the TOF between the B0 and the degrader counters for different particles and for the various beam momenta. The summary of this search is illustrated in fig. 1.
It is clear that all three types of particles can be well separated based on their TOF. The separation, naturally, increases for the lower momenta but so does the intensity of the pion beam. At this point the nominal momentum for the running was chosen to be 75 MeV/c. In addition to the TOF separation we can discriminate particles based on the energy deposited in the degrader and partially in the target. The corresponding distributions for the 75 MeV/c beam momentum are shown in fig. 2. The bottom plot of fig. 2 displays a double "hump" in the pion energy distribution. The target ADC in our experiment was a prompt ADC, i.e., it integrated the signal within a $\sim$50 ns gate immediately following the pi-stop signal (a coincidence between B0 and the degrader counter). Thus, first "hump" corresponds to a pion stopping in the target while the second feature is a sum of the original pion and the decay muon if it decayed within the ADC allowed gate. provided a $\sim$26 ns pion life time we see that majority of the pions have decayed. It also tells us that the muon signal in the target is of the considerable size to be nicely distinguished from the pion signal in the target.
After these simple tests the setup was slightly modified by introducing the NaI crystal to the system and by replacing our simple target by a faster one built in the UniZuri shop. The TOF separation remained unchanged as well as the energy depositions in the degrader. This is best illustrated in fig. 4. Notice that due to the relatively large suppression of the pions compared to

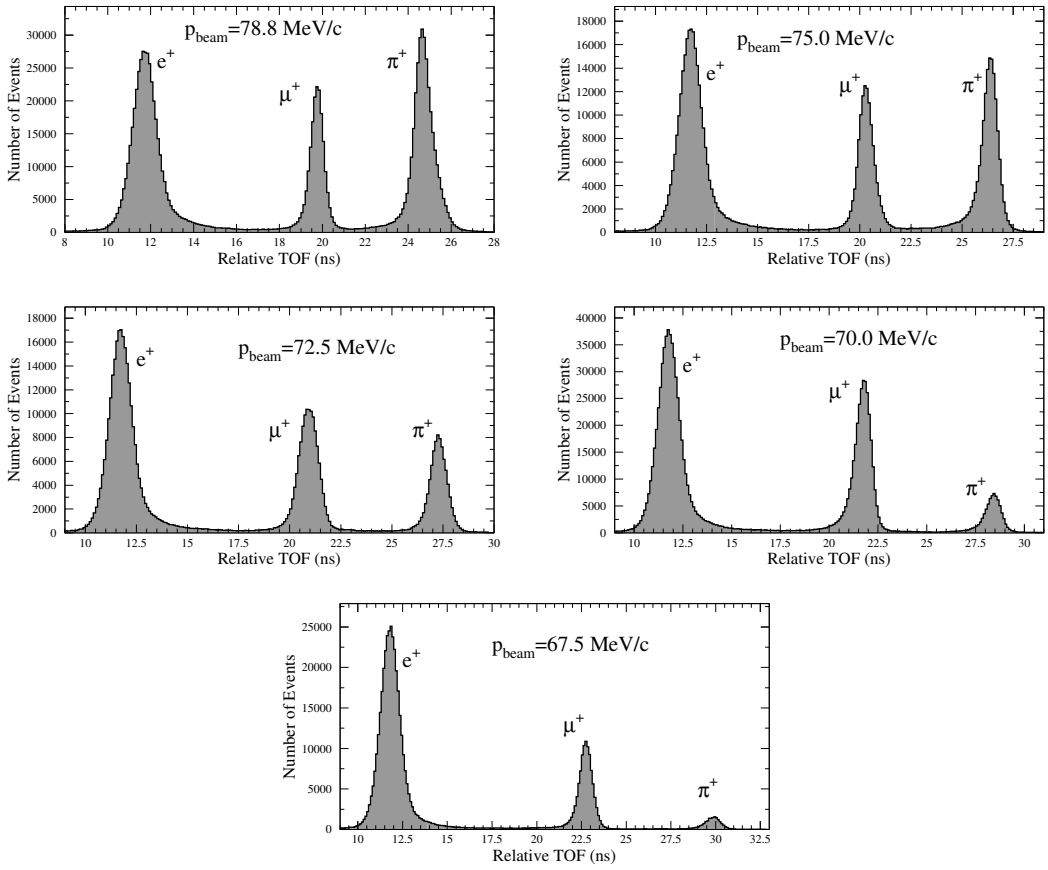

Figure 1: TOF difference for beam positrons, muons and pions for different beam momenta.

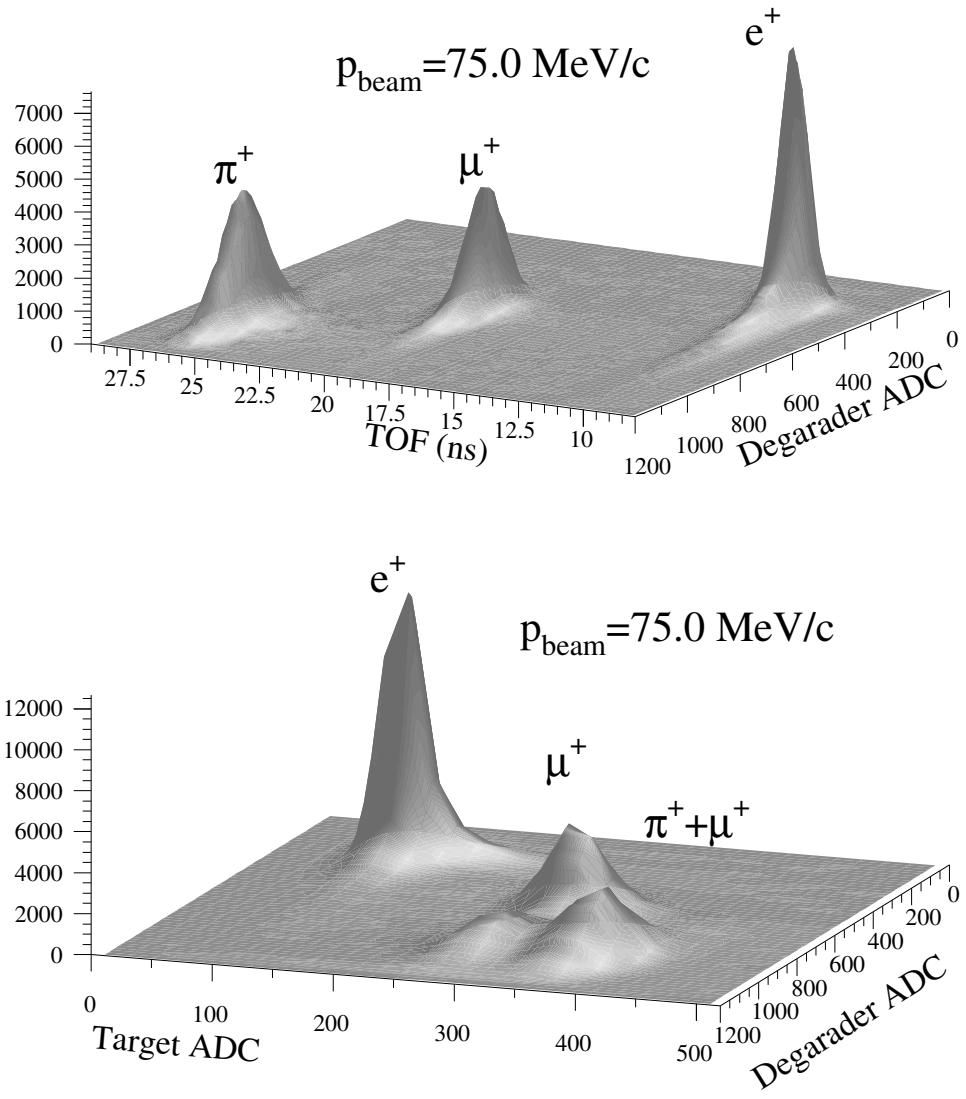

Figure 2: Energy deposited in the degrader vs. TOF (top panel) and energy in the degrader vs. energy deposited in the target (bottom panel).

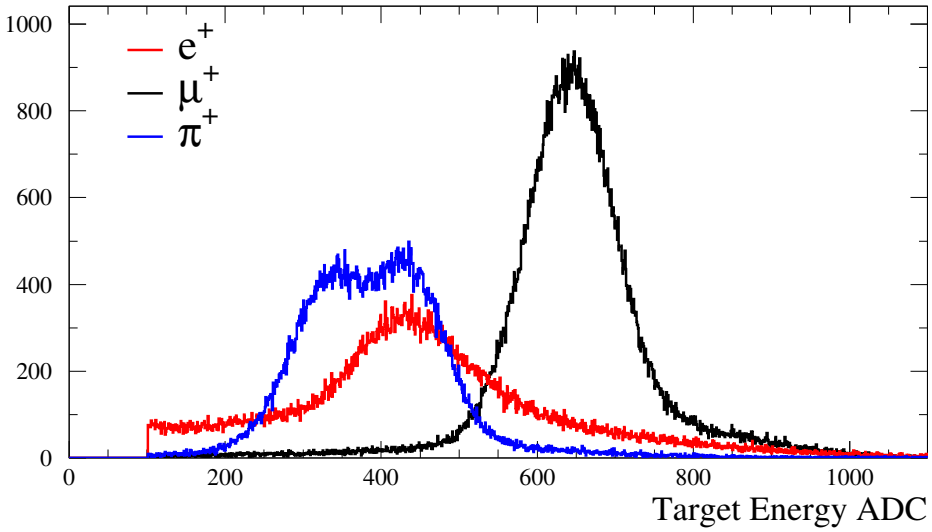

Figure 3: Energy deposited in the target for the setup with UniZuri target and NaI crystal implemented.

the positrons this histogram is not drawn to scale, i.e., the heights of the peaks are arbitrarily normalized.
The next step was to analyze the energy depositions in the new target for different particles based on the TOF and energy deposited in the degrader information. An additional cut is made on the relative times of the two B0 PMTs, degrader-target TDC signals and counter6-NaI signals, i.e., it is required that the TDC hits in these pairs are correlated. This cut significantly suppresses prompt background and accidental coincidences. The result is shown in fig. 3. Notice significant suppression of the beam positron events. It is achieved by requiring a valid TDC hit in the NaI calorimeter which only keeps events with large scattering angles in the target.
An important feature of the plot in fig. 3 is that 75 MeV/c positrons have very long high energy tail which indicates an expected behavior of the $\pi \to e\nu$ positrons. The double "hump" in the pion signal is still visible even though the light output of the new target is not as strong.
The pion target energy requires an additional short discussion. As it was mentioned earlier, target ADC gate is a prompt signal immediately following the pi-stop signal. The length of the ADC gate is $\sim$ 50 ns which assures

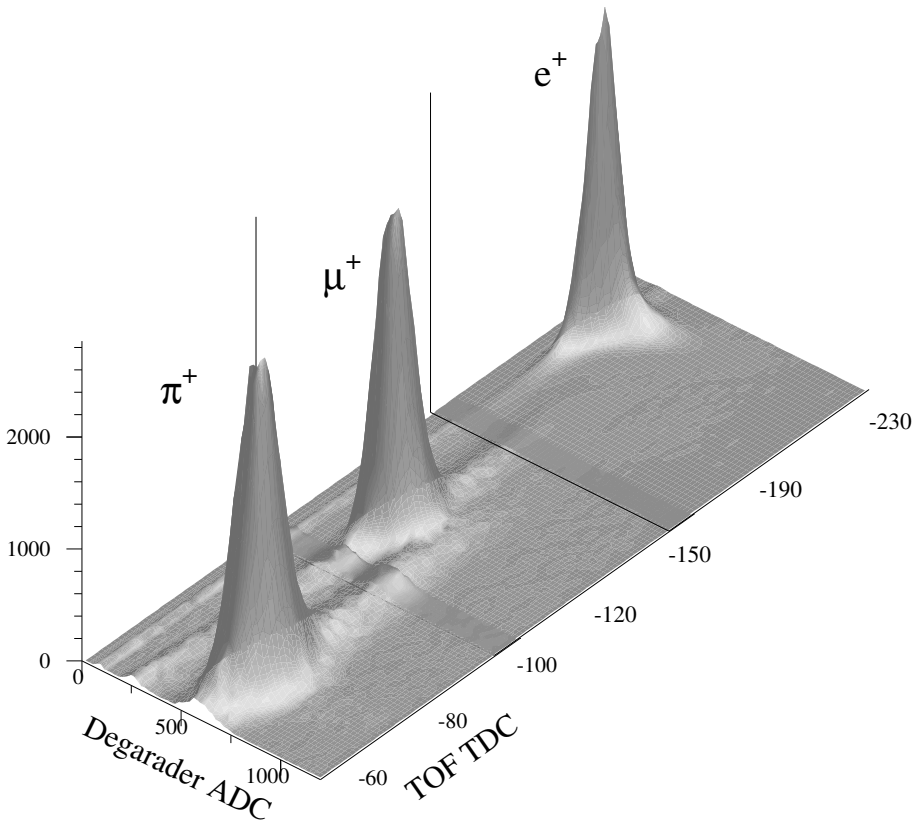

Figure 4: Energy deposited in the degrader vs. TOF for the setup with UniZuri target and NaI crystal implemented.

that the pion signal is always integrated by the ADC. The decay products, however, might not be integrated by the ADC if the decay occurred after the end of the ADC gate. If we want to extract the energy of the decay positrons or muons we should only consider early decays where this information can be recovered from the target energy. For the later decays target ADC only contains the stopping pion energy and does not add anything to the overall energy resolution. This point is illustrated in fig. 5. In this case the decay time is measured as the difference in TDC values between the target and counter6. In addition low energy deposited in NaI is requires to have a valid decay particle in the calorimeter. As expected the decay time distribution exhibits a time structure of the dominant $\pi \rightarrow \mu \rightarrow$ e chain and the target energy projections is a familiar double "hump". What is important is that we only see a variation in the target energy spectrum for the early times while for the later times it is nearly a constant.
Before we proceed to discuss the NaI spectra for different particles it is worth looking into the TDC/ADC spectra of the counter6 and see if it provides us with any additional information about the decay particles. Fig. 6 shows the time difference between the counter6 and the target (decay time) for different types of particles. The plots require a NaI energy above very low threshold. All three plots look exactly as expected. Top plot (note the logarythmic scale) is dominated by the prompt positrons which are scattered beam positrons with a very flat background. The plot in the middle is very long exponential curve of the muon decaying into positrons. The bottom plot is already familiar $\pi \rightarrow \mu \rightarrow$ e chain of decays with a characteristic shape.
The ADC spectra of the counter6 look nearly indistinguishable and are shown in fig. 7. This is to be expected since nearly all the particles traversing counter6 are minimum ionizing positrons independent of the parent process or particle.
A very interesting piece of information can be extracted from the counter6 ADC spectrum around the prompt time requiring high energy depositions in the NaI and pion TOF. This spectrum is shown in fig. 8. We can see heavier particles at the pi-stop time which deposit much more energy in counter6. In particular we can require the counter6 energy to be below a certain threshold to further suppress prompt particles in out detector.

At this point we have enough information to extract the $\pi \rightarrow e\nu$ events from our data set. Let us summarize the main cuts used for this procedure:

- Require pion TOF as defined in fig. 4.

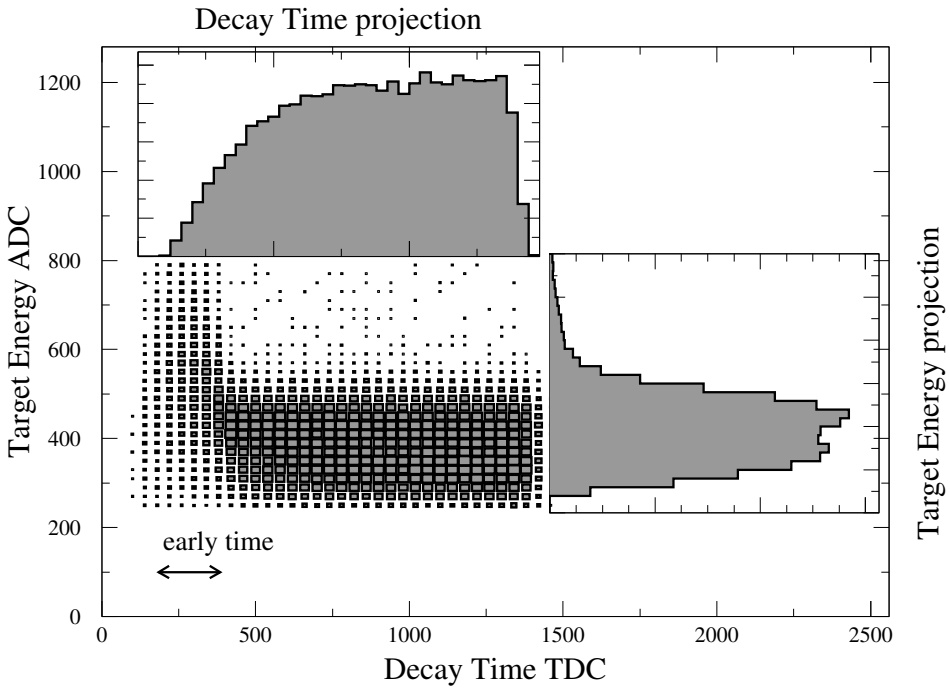

Figure 5: Energy deposited in the target vs. decay time measured as the time difference between the target and counter6. Only early times contain the decay positron energy due to the prompt target ADC.

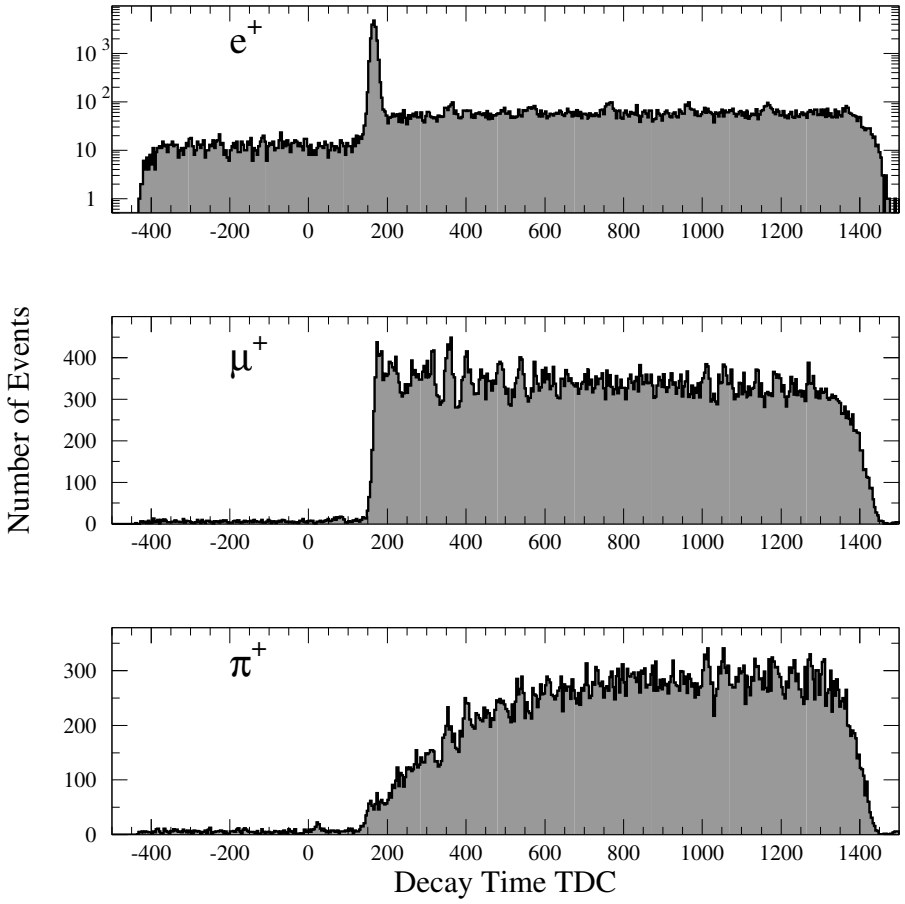

Figure 6: Decay times for different types of beam particles: from top to bottom positrons, muons and pions.

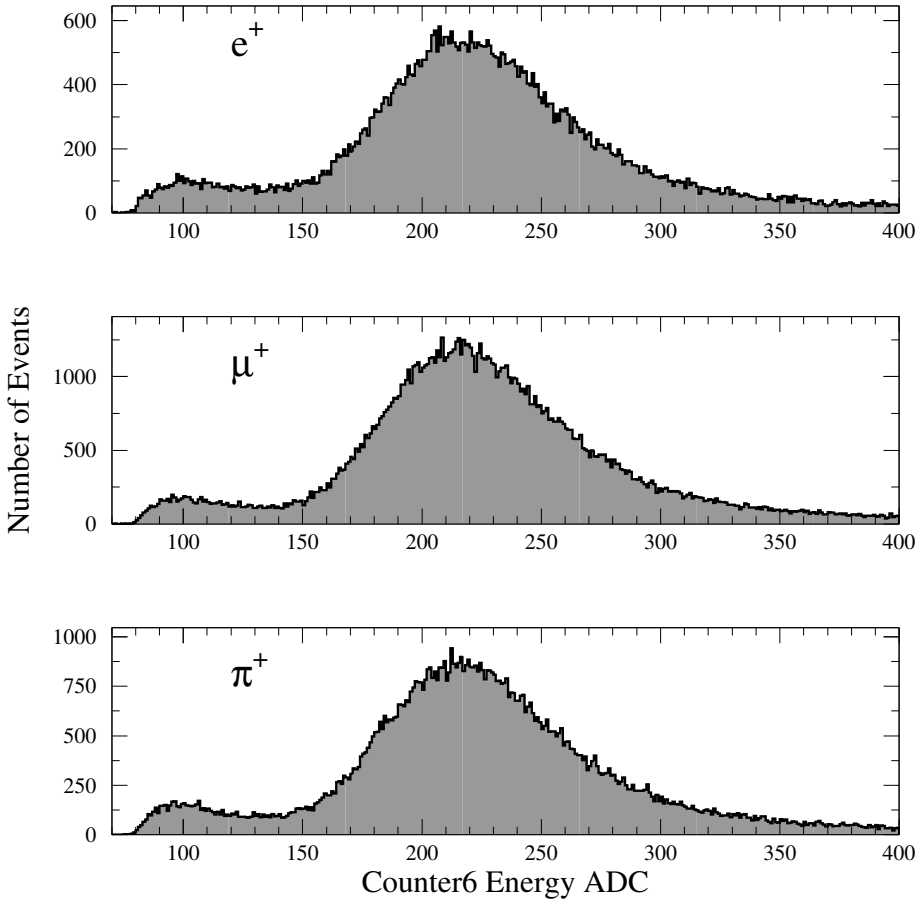

Figure 7: Energy deposited in the counter6 for different types of beam particles: from top to bottom positrons, muons and pions.

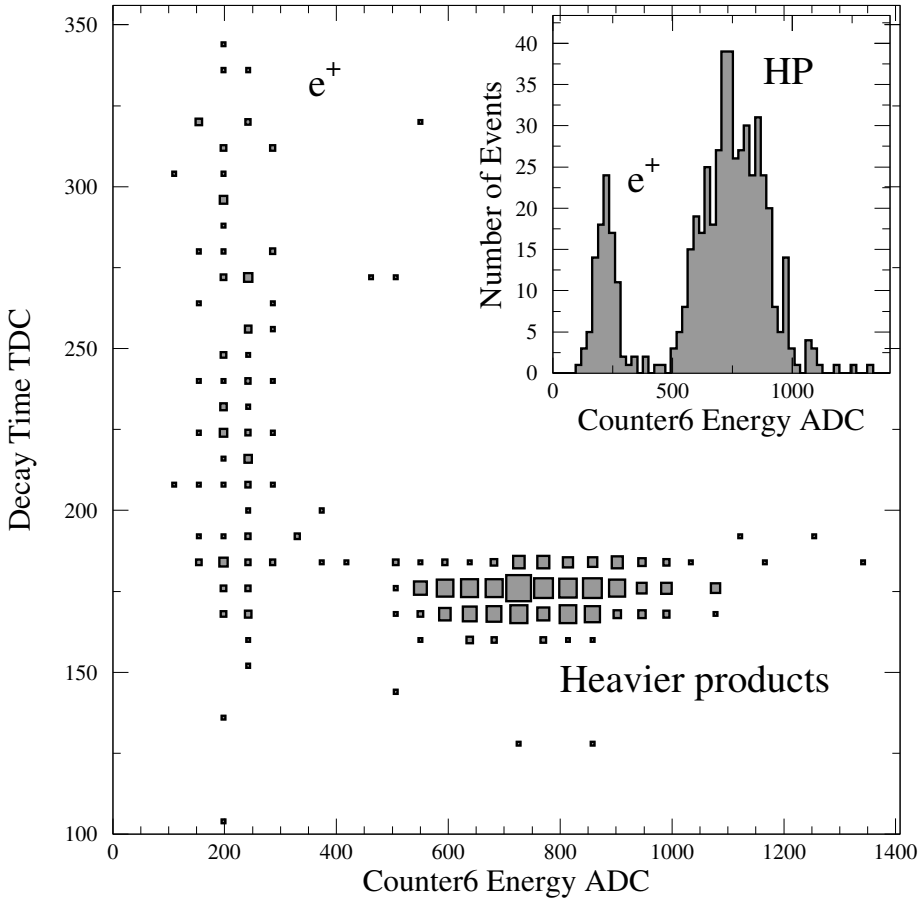

Figure 8: Energy deposited in the counter6 cut on the pion TOF and high energy in the calorimeter shows two peaks. The second one is due to the heavier products of the strong interaction: scattered pions and protons.

- Require appropriate to pions energy depositions in the degrader and the target as defined in fig. 4 and fig. 3.

- Require only early decay time in the total energy as shown in fig. 5. This serves two purposes. Firstly the correlation between the NaI energy and the target energy remains only for early times. Secondly we expect to suppress $\pi \rightarrow \mu \rightarrow$ e chain decays with very long muon lifetimes (see fig. 6) compared with the short pion lifetime.

- Require low energy depositions in counter6 as shown in fig. 8. This additionally suppresses the heavier products of the pion-nucleus prompt interactions.

- Require low energy threshold on the NaI energy to suppress beam scattered positrons and accidental background and to further suppress low energy $\pi \rightarrow \mu \rightarrow$ e chain decays.

The resulting total energy spectrum is shown in fig. 9. On the main plot we can clearly distinguish $\pi \rightarrow e\nu$ positron peak from the continuous Michel spectrum. On the insert the red line shows correlation of the target energy and NaI energy. The slope of this line is -0.14 and it serves as a relative normalization of the NaI and target ADCs.
Time spectra corresponding to the high and low NaI energies (denoted as region I and II on the insert of the fig. 9) are shown in fig. 10. As expected the first plot displays an exponential curve with pion lifetime. Second plot is already familiar chain decay spectrum.

Lastly, we can discuss the implementation of the waveform digitizer. The target digitizer system is implemented using the digital LeCroy oscilloscope which is read by the MIDAS front end and is fully integrated within the MIDAS analyzer system. It is known that our new target did not perform to the required specifications. Due to the loss of the amplifiers it is quite noisy and produces the waveforms of relatively low quality. We can try to perform very easy tests of the system. We can extract the candidates ror our $\pi \rightarrow e\nu$ events from the analog data by requiring a valid event with high energy in the NaI. We expect to see a very simple waveforms made of two peaks: the pion stop peak and the decay positron peak. After analyzing an entire run60612 there were 17 valid candidates for our decay.

In order to separate two peaks in the digitizer waveform we must first prepare a system function. A system function describes a typical signal in

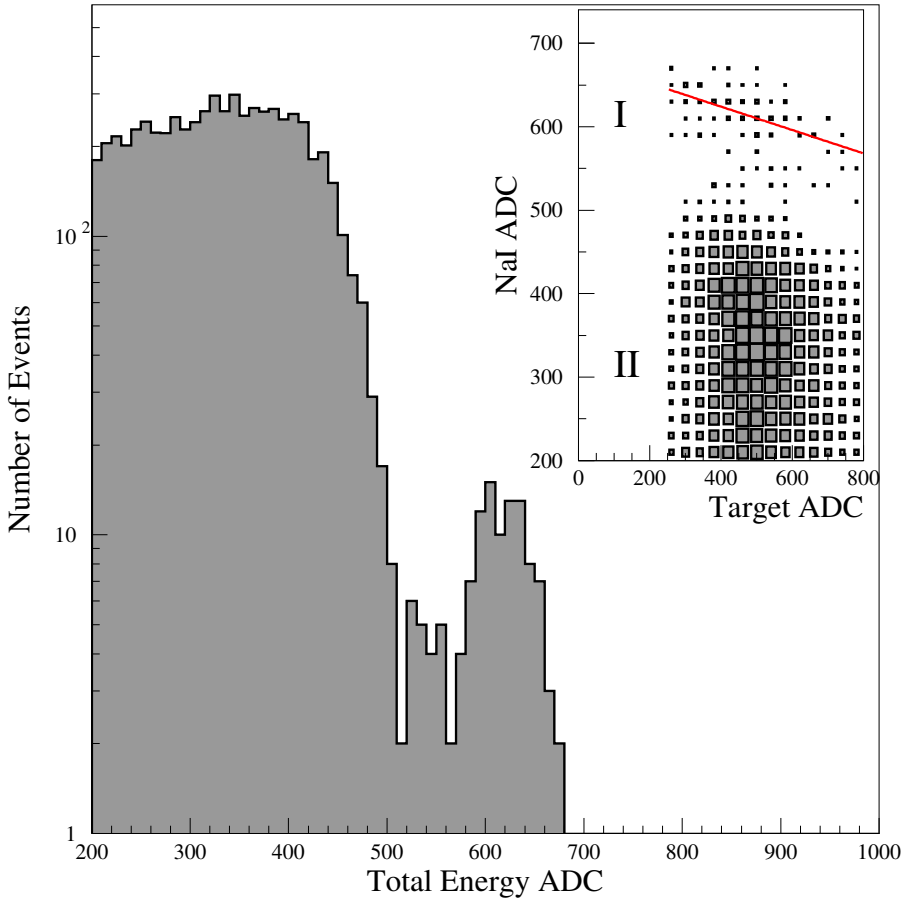

Figure 9: Energy deposited in the NaI plus energy in the target for the select pion events (main plot) and the NaI energy vs. target energy for the same events (insert).

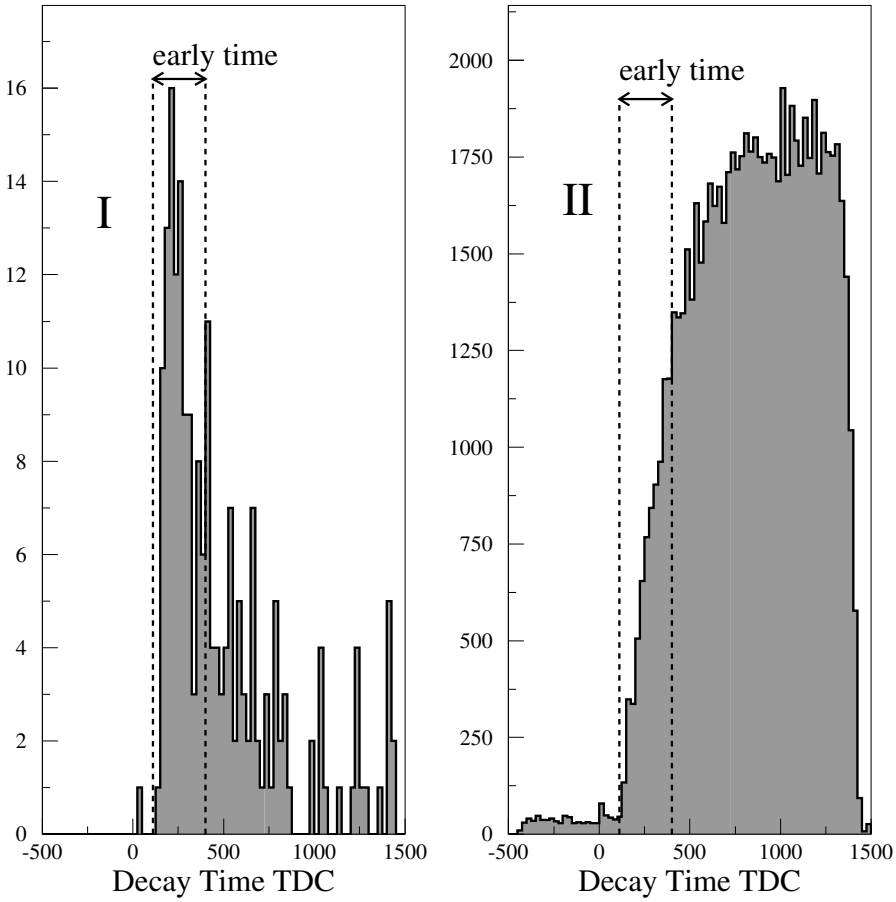

Figure 10: Time spectra for the high and low energy depositions in the NaI for the select pions. The arrows indicate the early time window used in the analyzes.

our target produced by a single particle. Subsequently, the entire digitizer waveform can be fitted with any linear combination of such system functions. The physicsl parameters, such as decay times and target energy can be extracted from the individual components of the fit. Fig. 11 shows few select waveforms and the corresponding fits. Arrows indicate the decay time found from the fits to the waveforms. Notice that our algorythm correctly identifies a double peak events even in very difficult cases (bottom of fig. 11).
Next plot (fig. 12) shows the correspondence between the digital and analog data. We have plotted the decay time from the TDC data versus the decay time extracted from the waveform fits for the same events. The agreement is rather reasonable for all 17 events in question.

A similar procedure can be performed for the $\pi \to \mu \to$ e chain events. Based on the energy in NaI data we picked 40 chain event candidates. Two select waveforms and the fits are shown in fig. 13. Again, the fitting procedure correctly handles very difficult waveforms.

Fig. 14 shows the match between the analog and digital data. Three evnts are clearly missidentified. All three events correspond to the low energy deposition by a positron when it can not be correctly separated from the noise.

3 Additional remarks

The digitizer analysis requires more work. A better system funcion and such...

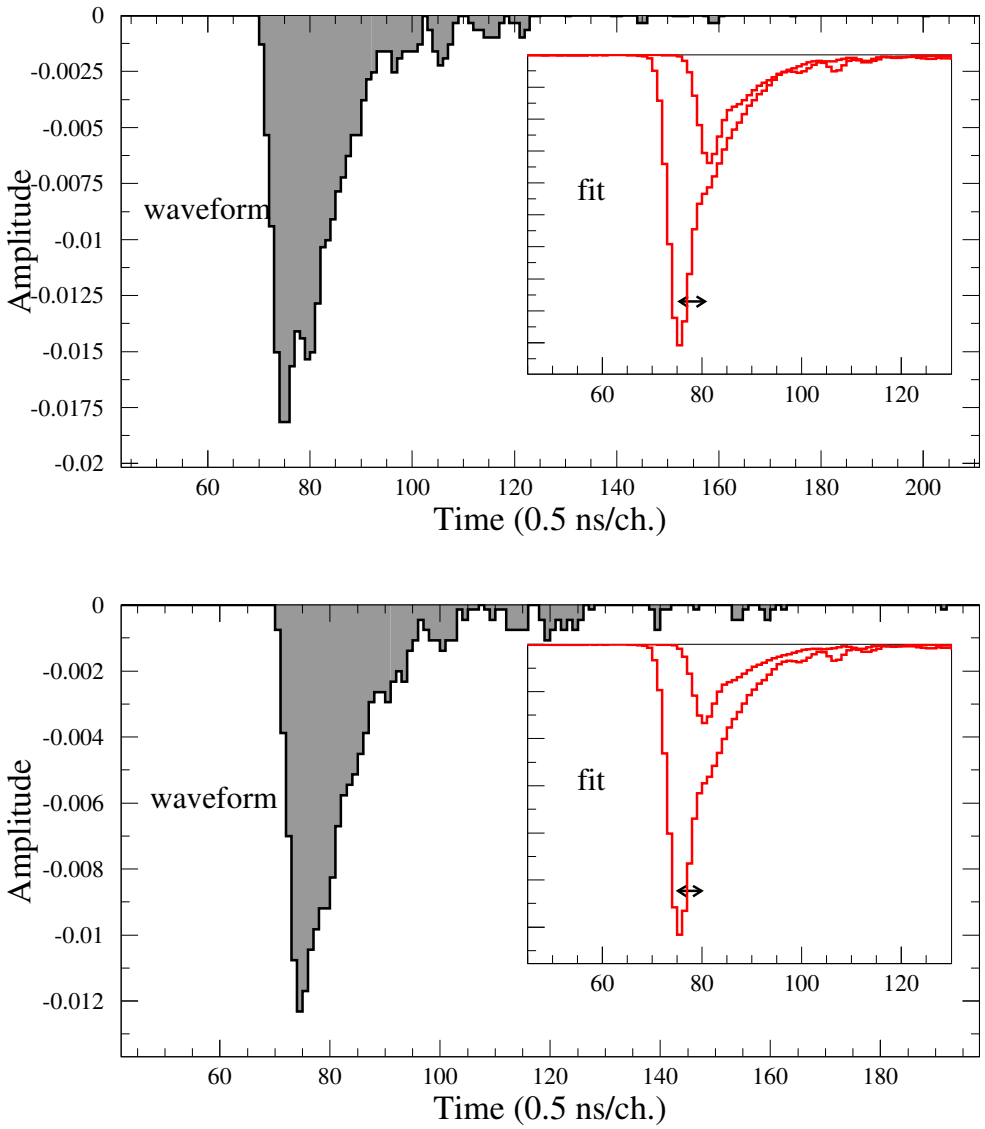

Figure 11: Select waveforms shown as histograms. The inserts show the fits to the waveforms. Arrows indicate the decay time found from the fits.

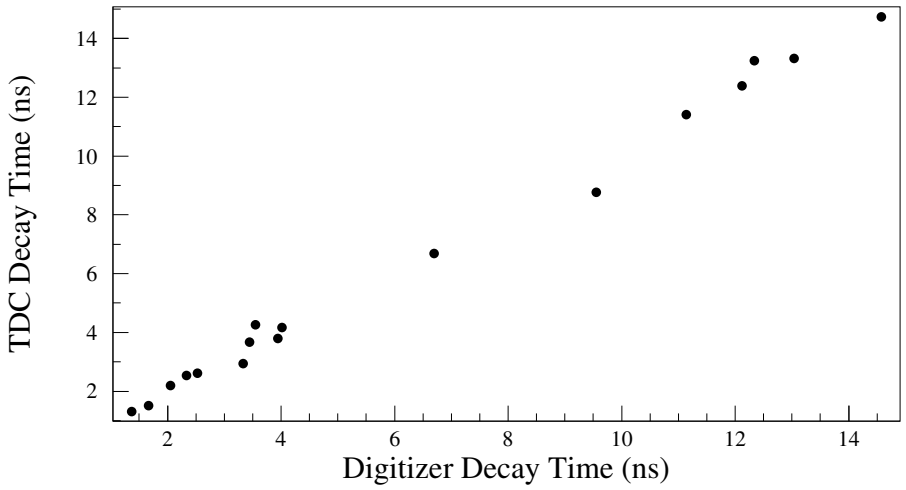

Figure 12: The match between the TDC and the digitizer data for $\pi \rightarrow e\nu$ candidates.

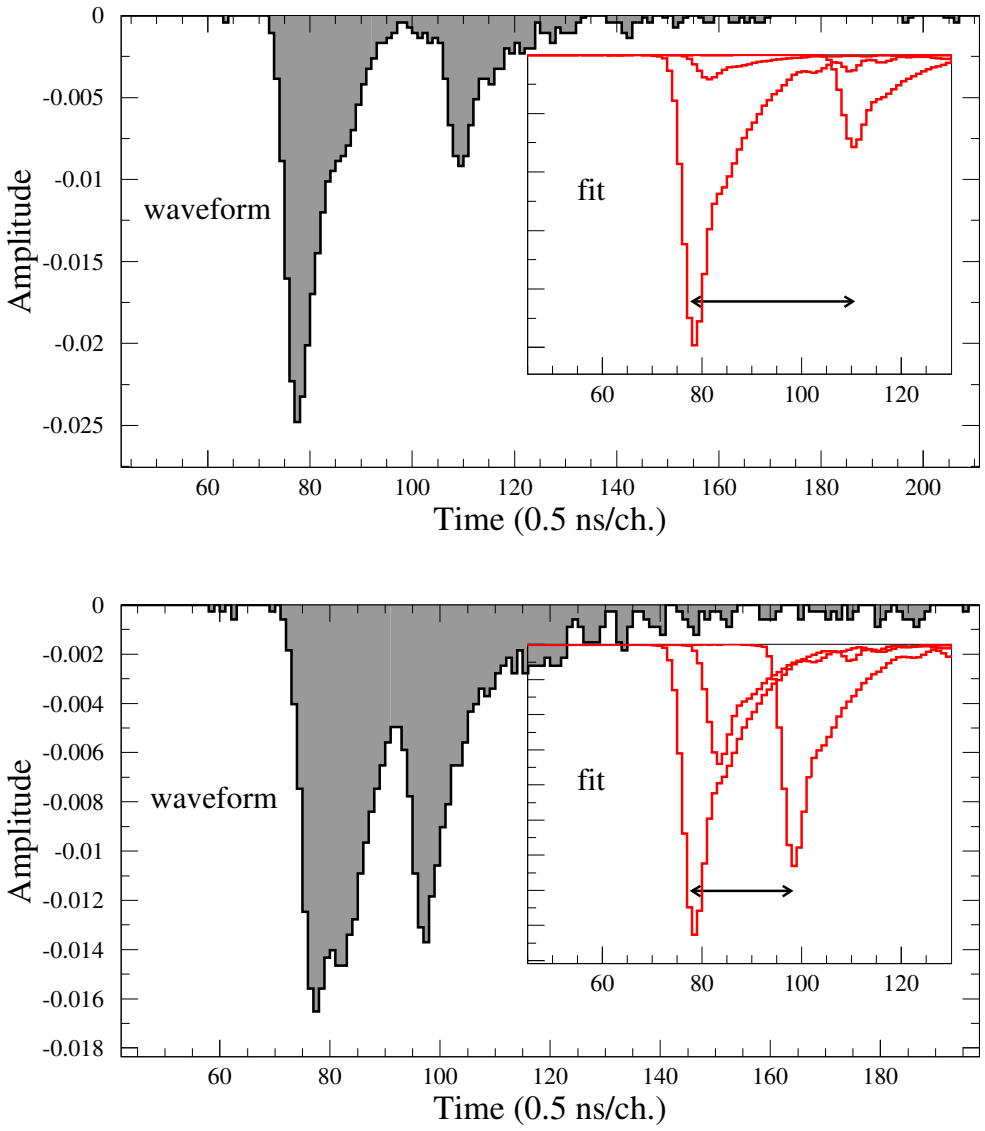

Figure 13: Select waveforms shown as histograms. The inserts show the fits to the waveforms. Arrows indicate the decay time found from the fits.

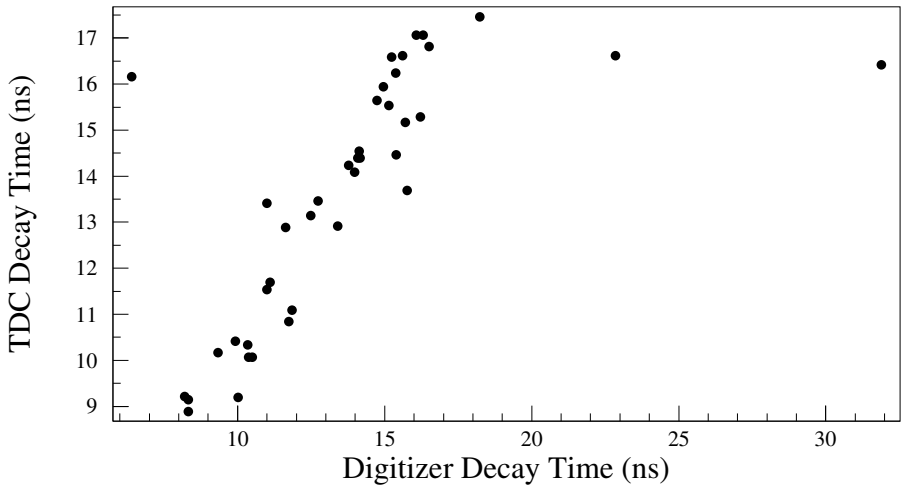

Figure 14: The match between the TDC and the digitizer data for $\pi \rightarrow \mu \rightarrow$ e candidates.